Multi-scale spatial correlation and scaling behavior of surface soil moisture

Dongryeol Ryu[1] and James S. Famiglietti[1]

Received 23 January 2006; revised 5 March 2006; accepted 20 March 2006; published 26 April 2006.

[1] The scaling behavior of surface soil moisture variance is presented across spatial scales of observation from 1 × 1 km^2 to 140 × 140 km^2. Semi-variograms were used to analyze the spatial correlation in remotely sensed soil moisture data from SGP97. Results indicate that a nested correlation structure exists within regional scale fields. Three representative semi-variograms were chosen to calculate the scaling of soil moisture variance with increasing support scale. While previous research at smaller scales (<1 km^2) revealed that soil moisture variance follows a power law decay with increasing support area, we show that in the presence of significant spatial correlation at the larger scales studied here, a power law relationship no longer holds. Rather, the type of correlation function and correlation length play an important role in the relationship between soil moisture variance and support area. We suggest that understanding the spatial correlation pattern of soil moisture across scales is critical for characterizing the scaling behavior of soil moisture variance. **Citation:** Ryu, D., and J. S. Famiglietti (2006), Multi-scale spatial correlation and scaling behavior of surface soil moisture, *Geophys. Res. Lett.*, *33*, L08404, doi:10.1029/2006GL025831.

1. Introduction

[2] Surface soil moisture plays a key role in the exchange of energy and water between the atmosphere and the land surface. Realistic spatial representation of soil moisture can improve the representation of land surface processes in hydrologic and general circulation models, including evapotranspiration and runoff [*Famiglietti and Wood*, 1994], dust emission [*Fécan et al.*, 1999], and the predictability of precipitation [*Koster et al.*, 2000] and mesoscale circulations. In response to the need for characterization of global scale soil moisture distributions, current and future spaceborne microwave sensors will be producing 40- to 60-km footprint-scale surface soil moisture estimates across the globe [*Famiglietti*, 2004]. However, due to the nonlinear relationship between land surface processes and soil moisture, disregarding sub-footprint-scale heterogeneity of soil moisture can lead to inaccurate prediction of the atmospheric circulation or bias in the pixel-aggregated model outputs [*Giorgi and Avissar*, 1997].

[1]Department of Earth System Science, University of California, Irvine, California, USA.

0094-8276/06/2006GL025831

[3] Subgrid-scale heterogeneity of soil moisture is often represented by the variance of soil moisture within a region. When dealing with the soil moisture variance, three observation scales of soil moisture should be considered; spacing, support, and extent [*Blöschl and Sivapalan*, 1995; *Western and Blöschl*, 1999]. Spacing refers to the distance between measurements or data points. Support refers to the effective area or volume which the measurement represents. Extent is the total size of the spatial domain. For example, for the case of a 50 × 50 km^2 remote sensing footprint divided into 2500 1 × 1 km^2 grids, the extent scale is 50 km and the support scale is 1 km. Within a large region, the total soil moisture variance (see section 4) is the sum of the variance of the measurements at the support scale (e.g., of the subgrids) and the variance within the support scale (e.g., within the subgrids). The focus of this work is on the scaling behavior of soil moisture spatial variance with increasing support scale, in the context of increasing subgrid size within remote sensing footprints or any larger region. *Famiglietti et al.* [2006] discuss the behavior of soil moisture variance with increasing extent scale.

[4] *Rodríguez-Iturbe et al.* [1995] reported that, for a fixed extent scale, the log variance of soil moisture decreases linearly with increasing log support scale, or follows a power law decay. *Hu et al.* [1998] and *Crow and Wood* [2002] suggested further that this relationship provides a framework for downscaling soil moisture variance from remote sensing footprints to subgrids of a given support scale within the footprint.

[5] We believe that the effective range of the spatial scales within which the *Rodríguez-Iturbe et al.* [1995] power law holds must be carefully examined, because the linear trends may hold only within the correlation length of the soil moisture spatial distribution [*Levin*, 1992]. *Rodríguez-Iturbe et al.* [1995] explored relatively small support scales, from 30 × 30 m^2 to 1 × 1 km^2, within which only one correlation length may be apparent. However, surface soil moisture content is spatially correlated with multiple correlation lengths ranging from a few tens of meters [*Anctil et al.*, 2002] to a few tens of kilometers, or even longer than a hundred kilometers [*Oldak et al.*, 2002; *Vinnikov et al.*, 1999]. This implies that there may exist a nested spatial correlation structure of surface soil moisture with more than one correlation length scale, resulting in multiple slopes of the power law decay pattern of soil moisture variance.

[6] Here we examine the scaling behavior of surface soil moisture spatial variance with increasing support scale, from approximately 1 × 1 km^2 to 140 × 140 km^2. In particular, we examine how the spatial correlation pattern of soil moisture, obtained from airborne remotely sensed

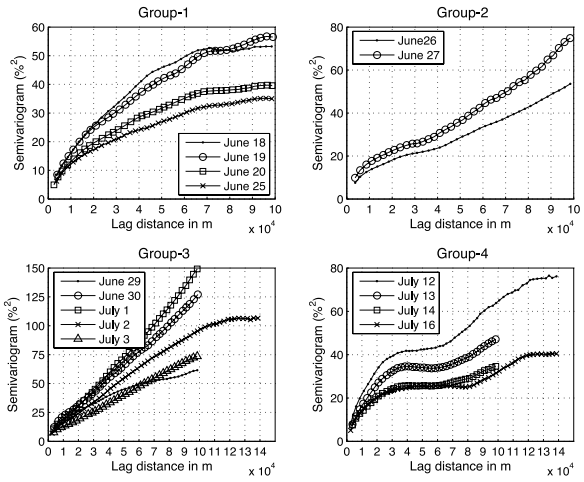

Figure 1. Semi-variograms of surface soil moisture derived from remotely sensed soil moisture data during SGP97. Groups 1–4 represent the four major drying sequences of the experiment.

images, influences the scaling behavior of the surface soil moisture variance and the log-linearity of the variance-support scale relationship.

2. Description of Data

[7] Airborne remotely sensed images collected during the Southern Great Plains 1997 (SGP97) Hydrology Experiment [*Jackson et al.*, 1999] were employed for the analyses in this work. The SGP97 experiment was conducted from June 18 to July 17, 1997 in a 50-km by 250-km region of central Oklahoma. During the experiment, the Electronically Scanned Thinned Array Radiometer (ESTAR), onboard a NASA P3B aircraft, collected sixteen daily soil moisture images at 800-m resolution over the region. The ESTAR data represent the surface soil moisture content in the top 5-cm soil layer with errors on the order of 3% compared to ground-based validation samples.

[8] During the experiment, there were roughly four major drying sequences; June 18 $\sim$ 25, June 26 $\sim$ 27, June 29 $\sim$ July 3, and July 11 $\sim$ 16. Each drying sequence started with partial wetting of the SGP97 region by rainfall events with length scales varying from 60- to more than 100-km [*Oldak et al.*, 2002].

3. Spatial Correlation

[9] In order to identify the spatial correlation in the SGP97 region, semi-variograms were calculated using the daily ESTAR data. Since the dimension of the experiment region was highly anisotropic, each pair of measurements for the semi-variogram was chosen along the longer dimension. The longest lag distance is typically 100 km, which is approximately one third of the longer dimension of the study region. Due to the large number of pixels within each image, the number of semi-variogram pairs is over one million even at the largest lag distance. In addition, the ESTAR mapping region was extended by about 130 km to the north on a few days, which allowed us to increase the maximum lag distance to 140 km on July 2, 12, and 16, 1997.

[10] Figure 1 displays semi-variograms during each of the four major drying sequences of SGP97, named Groups 1 $\sim$ 4. The overall spatial correlation pattern is characterized by the existence of at least two correlation lengths. Shorter correlation lengths have variogram ranges from about 10 to 30 km. Longer correlation lengths display variogram ranges from about 60 to 100 km or larger. The longer variogram ranges are attributed to large-scale rainfall events, while the shorter ranges are related to the spatial pattern of soil texture within the SGP97 region [*Kim and Barros*, 2002; *Oldak et al.*, 2002]. An analysis of the normalized difference vegetation index (NDVI) reveals that the semi-variogram ranges of the vegetation density in the Southern Great Plains also fall between 20 and 40 km [*Cosh et al.*, 2003].

[11] In Groups 1 and 3 of Figure 1, spatial correlation patterns of soil moisture are dominated by rainfall patterns with large correlation scales, although the semi-variograms show slight inflections around a lag distance of 10 km. This is likely a consequence of the soil texture within the larger scale wet and dry patches of the soil moisture fields. In Group 3, most of the semi-variograms do not display sill within the maximum lag distance, a result of the gradual increase in surface wetness from south to north (see the soil moisture images shown by *Jackson et al.* [1999]). However, when the maximum lag distance was extended to 140 km due on July 2, 1997, a sill was observed at about 140 km. In Group 2, whereas a sill was observed with a variogram range of roughly 30 km, which also resulted from the spatial pattern of soil texture, the major correlation patterns result from the large-scale rainfall event of June 25. In Group 4, there are two distinct correlation scales, one with a range between 30 and 40 km and the other with about 120 km. The observed nested correlation patterns result from the combined effect of land surface features (i.e., soil texture and vegetation water content) and the spatial pattern of rainfall [*Kim and Barros*, 2002].

4. Semi-Variogram and Scaling Behavior

[12] Within a specific range of spatial scales, the variance of surface soil moisture follows a power law decay [*Rodríguez-Iturbe et al.*, 1995], that is, the log variance of soil moisture decreases linearly with increasing log support scale. The slope of the power law decay is determined by the spatial correlation pattern of soil moisture, from -1 for independent random variables to 0 for the completely correlated variables [*Hu et al.*, 1997]. Given the semi-variogram of a soil moisture field, the functional relationship between log variance and log support scale can be reproduced using the regularization technique [*Journel and Huijbregts*, 1978; *Western and Blöschl*, 1999]. If we know the true variance of the soil moisture field, σ^2_{true}, then the variance at the support scale of s, σ^2_s, can be calculated as:

$$\sigma^2_s = \sigma^2_{\text{true}} - \sigma^2_{\text{within } s}, \tag{1}$$

where $\sigma^2_{\text{within } s}$ is the soil moisture within the support scale. In the regularization technique, $\sigma^2_{\text{within } s}$ is calculated using the given semi-variogram of the field and the probability density function of the distances between two points within

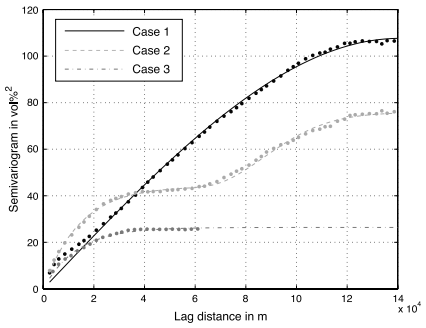

Figure 2. Three representative cases of spatial correlation constructed based on the observed spatial distributions of soil moisture during SGP97. Black and gray dots are semi-variograms calculated using ESTAR soil moisture images as in Figure 2, and the lines are fit curves.

the support, and the spatial correlation is assumed to be isotropic within the support. More details of the calculation are given by *Western and Blöschl* [1999, appendix]. Note that direct aggregation of soil moisture pixels is also a viable approach to compute the variance at the support scale. However, the highly anisotropic shape of the ESTAR domain would greatly limit the maximum support scale that could be analyzed in this work.

[13] Based on the calculated semi-variograms in Figure 1, three cases were chosen as the representative spatial correlation patterns of surface soil moisture (Figure 2). Case 1 represents the case where the soil moisture spatial correlation pattern is determined predominantly by rainfall. A spherical model was fit to the semi-variogram on July 2 for Case 1. Case 2 represents the case where the spatial correlation pattern of soil moisture is influenced by both large-scale rainfall and small-scale land surface features such as soil texture and vegetation. The nested semi-variogram of July 12 was chosen to represent Case 2. In order to fit the nested structure, two semi-variogram models were fit to the two separate ranges of the lag distance, respectively. An exponential model was used for the lag distances from 0 to 60 km, and a Gaussian model was fit to the data with lag distances from 60 km to 140 km. Case 3 assumes that, after some period of drying, the soil moisture correlation pattern mostly represent soil texture and vegetation features. Part of the semi-variogram for July 14, with lag distance from 0 to 60 km, was used to construct the exponential model for the Case 3. Parameters of the semi-variogram models for the Cases 1 $\sim$ 3 are summarized in Table 1.

5. Scaling Behavior of Soil Moisture Spatial Variance

[14] Figure 3 displays the scaling behavior of soil moisture variance with increasing support scale. Each case was reproduced by applying the regularization technique to the corresponding semi-variogram models in Figure 2. True variances were taken as the variances of the soil moisture images on July 2, 12, and 14 at the 800-m scale. For simplicity, we ignore the variance within the 800-m scale [*Famiglietti et al.*, 1999], which would likely increase the true variances reported here.

Table 1. Summary of Semi-Variogram Ranges[a] and Variances[b]

	First Range	Second Range	σ^2 at 1×1 km^2	σ^2 at 140×140 km^2
Case 1	140622	—	93.55	23.09
Case 2	14287	97573	81.12	31.42
Case 3	13165	—	31.72	7.47

[a]Unit is in meters.
[b]Unit is in %^{2}.

[15] Soil moisture variance decreases from Case 1 to Case 3 because of the corresponding decrease in mean moisture content across the entire region, which reduced the large-scale north-south soil moisture gradient during the drydown. Also, the ESTAR image on July 14 did not include the extended (wet) region present in the images of July 2 (Case 1) and July 12 (Case 2).

[16] In all cases, log variances show a fairly linear trend until the support scale reaches about 2×10^8 m^2, approximately a 14 km length scale. However, in Cases of 2 and 3, the slopes of the curves become noticeably steeper after the length scale of the support exceeds the ranges of semi-variograms (shown as vertical dashed lines). In Case 2, the slope of the scaling curve becomes steeper once again after the second range of the nested variogram is exceeded. This implies that in the case of spatially organized variables with exponential or Gaussian semi-variograms, the variogram range could be used as a measure of the length scale at which the linear trend between log variance and log support scale changes.

[17] On the other hand, in Case 1, nonlinearity of the log variance curve appears sooner than in Cases 2 and 3 relative to the variogram range, which in this case is about 140 km. This suggests that, not only the correlation length of the spatial variable, but also the shape of the semi-variogram function may have an important influence on the decreasing trend of log variance with increasing support scale. The spherical semi-variogram increases more monotonically than the exponential or Gaussian models. Although the variance of Case 1 is larger than Case 2 at the support scale of 1 km, it decreases to a smaller value than Case 2 at the 140-km scale (Figure 2 and Table 1).

6. Discussion and Conclusions

[18] At least two different scales of spatial correlation are observed in the SGP97 soil moisture field. Smaller scale correlation (10 $\sim$ 30 km) is caused by slowly or non-

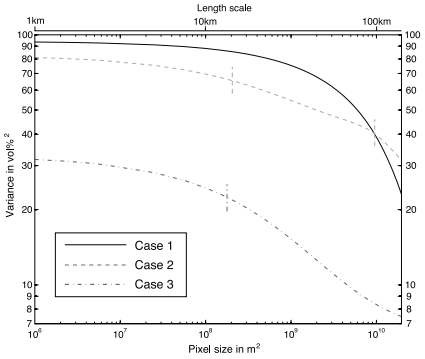

Figure 3. Surface soil moisture variance vs. support scale. Cases 1–3 are described in the text. The case numbers correspond to those in Figure 2. Vertical lines for Cases 2 and 3 mark the semi-variogram ranges.

changing land surface features like vegetation and soil texture, while larger scale correlation (60 $\sim$ 100 km and greater) results from precipitation, which is dynamic and more difficult to predict. By applying the regularization technique to three representative cases, which are based on the observed spatial distribution of soil moisture, it was shown that spatial variance of soil moisture does not follow a power law decay between the support scales of 1 km and 140 km, and depends on the spatial correlation characteristics of the soil moisture field. This range of spatial scale is particularly important because it includes the typical grid sizes of land surface and hydrological models, as well as soil moisture remote sensing products. For the case where correlation of soil moisture can be characterized by the exponential and/or Gaussian semi-variogram models, the linearly decreasing trend of log variance noticeably changes around the variogram range of each model.

[19] The existence of the multi-scale nested semi-variograms indicates that the decaying pattern of soil moisture variance with increasing support scale could be complex, composed of piecewise-linear sections bounded by distinct correlation lengths. In addition to the scales addressed in this work, *Anctil et al.* [2002] and *Kelly et al.* [2003] reported spatial correlation of surface soil moisture with variogram ranges between 30 and 65 m, which implies that the actual scaling behavior of soil moisture variance could be even more complex than that presented here.

[20] The power law decay of soil moisture suggested by *Rodríguez-Iturbe et al.* [1995] can also be understood in the context of spatial correlation. That study used soil moisture data collected during the Washita '92 experiment and identified the linear decrease of log variance with increasing log support scale from 30×30 m^2 to 1×1 km^2. According to *Cosh and Brutsaert* [1999], soil moisture fields observed during the Washita '92 experiment showed spatial correlation with the semi-variogram ranges of 1 km or longer, likely accounting for the linear decay of the soil moisture variance with increasing support scale found at the shorter length scales of the *Rodríguez-Iturbe et al.* [1995] study.

[21] This study strongly suggests that understanding the spatial correlation pattern of soil moisture is critical for predicting the scaling behavior of soil moisture variance. By identifying the range of support scales within which the linear decay of soil moisture variance holds, predicted scaling behavior can be utilized to parameterize the subgrid-scale soil moisture content as was suggested by *Crow and Wood* [2002]. More work is required to fully characterize the correlation lengths of the multiple environmental controls on soil moisture variability and their impacts on soil moisture variance across scales [e.g., *Isham et al.*, 2005].

[22] **Acknowledgment.** The support of NASA Earth System Science Fellowship grant (NNG04GQ53H) is gratefully acknowledged.

References

Anctil, F., R. Mathieu, L. E. Parent, A. A. Viau, M. Sbih, and M. Hessami (2002), Geostatistics of near-surface moisture in bare cultivated organic soils, *J. Hydrol.*, *260*, 30–37.

Blöschl, G., and M. Sivapalan (1995), Scale issues in hydrological modeling—A review, *Hydrol. Process.*, *9*, 251–290.

Cosh, M. H., and W. Brutsaert (1999), Aspects of soil moisture variability in the Washita '92 study region, *J. Geophys. Res.*, *104*, 19,751–19,757.

Cosh, M. H., J. Stedinger, and W. Brutsaert (2003), Time changes in spatial structure of surface variability in the Southern Great Plains, *Adv. Water Resour.*, *26*, 407–415.

Crow, W. T., and E. F. Wood (2002), The value of coarse-scale soil moisture observations for regional surface energy balance modeling, *J. Hydrometeorol.*, *3*, 467–482.

Famiglietti, J. S. (2004), Remote sensing of terrestrial water storage, soil moisture and surface waters, in *The State of the Planet: Frontiers and Challengers*, *Geophys. Monogr. Ser.*, vol. 150, edited by R. S. J. Sparks and C. J. Hawkesworth, pp. 197–207, AGU, Washington, D.C.

Famiglietti, J. S., and E. F. Wood (1994), Multiscale modeling of spatially variable water and energy balance processes, *Water Resour. Res.*, *30*, 3061–3078.

Famiglietti, J. S., J. A. Devereaux, C. A. Laymon, T. Tsegaye, P. R. Houser, T. J. Jackson, S. T. Graham, M. Rodell, and P. J. van Oevelen (1999), Ground-based investigation of soil moisture variability within remote sensing footprints during the Southern Great Palins 1997 (SGP97) Hydrology Experiment, *Water Resour. Res.*, *35*, 1839–1851.

Famiglietti, J. S., D. Ryu, A. Berg, M. Rodell, M. H. Cosh, R. Bindlish, and T. J. Jackson (2006), Field observations of soil moisture variability across scales, in preparation for Water Resour. Res.

Fécan, F., B. Marticorena, and G. Bergametti (1999), Parametrization of the increase of the aeolian erosion threshold wind friction velocity due to soil moisture for arid and semi-arid areas, *Ann. Geophys.*, *17*, 149–157.

Giorgi, F., and R. Avissar (1997), Representation of heterogeneity effects in Earth system modeling: Experience from land surface modeling, *Rev. Geophys.*, *35*, 413–438.

Hu, Z., S. Islam, and Y. Cheng (1997), Statistical characterization of remotely sensed soil moisture images, *Remote Sens. Environ.*, *61*, 310–318.

Hu, Z., Y. Chen, and S. Islam (1998), Multiscaling properties of soil moisture images and decomposition of large- and small-scale features using wavelet transforms, *Int. J. Remote Sens.*, *19*, 2451–2467.

Isham, V., D. R. Cox, I. Rodriguez-Iturbe, A. Porporato, and S. Manfreda (2005), Representation of space-time variability of soil moisture, *Proc. R. Soc., Ser. A*, *461*, 4035–4055, doi:10.1098/rspa.2005.1568.

Jackson, T. J., D. M. Le Vine, A. Y. Hsu, A. Oldak, P. J. Starks, C. T. Swift, J. D. Isham, and M. Haken (1999), Soil moisture mapping at regional scales using microwave radiometry: The Southern Great Plains Hydrology Experiment, *IEEE Trans. Geosci. Remote Sens.*, *37*, 2136–2151.

Journel, A. G., and C. J. Huijbregts (1978), *Mining Geostatistics*, 600 pp., Elsevier, New York.

Kelly, R. E. J., T. J. A. Davie, and P. M. Atkinson (2003), Explaining temporal and spatial variation in soil moisture in a bare field using SAR imagery, *Int. J. Remote Sens.*, *24*, 3059–3074.

Kim, G., and A. P. Barros (2002), Space-time characterization of soil moisture from passive microwave remotely sensed imagery and ancillary data, *Remote Sens. Environ.*, *81*, 393–403.

Koster, R. D., M. J. Suarez, and M. Heiser (2000), Variance and predictability of precipitation at seasonal-to-interannual time scales, *J. Hydrometeorol.*, *1*, 26–46.

Levin, S. A. (1992), The problem of pattern and scale in ecology, *Ecology*, *73*, 1943–1967.

Oldak, A., T. J. Jackson, and Y. Pachepsky (2002), Using GIS in passive microwave soil moisture mapping and geostatistical analysis, *Int. J. Geogr. Inf. Sci.*, *16*(7), 681–698, doi:10.1080/13658810210149407.

Rodríguez-Iturbe, I., G. K. Vogel, R. Rigon, D. Entekhabi, F. Castelli, and A. Rinaldo (1995), On the spatial organization of soil moisture fields, *Geophys. Res. Lett.*, *22*, 2757–2760.

Vinnikov, K. Y., A. Robock, S. Qiu, and J. K. Entin (1999), Optimal design of surface network for observation of soil moisture, *J. Geophys. Res.*, *104*, 19,743–19,749.

Western, A. W., and G. Blöschl (1999), On the spatial scaling of soil moisture, *J. Hydrol.*, *217*, 203–224.

J. S. Famiglietti and D. Ryu, Department of Earth System Science, University of California, Irvine, Irvine, CA 92697, USA. (jfamigli@uci.edu)